Engineer Research and Development Center

US Army Corps of Engineers®
Engineer Research and
Development Center

ERDC INNOVATIVE SOLUTIONS for a safer, better world

ERDC Center-Directed Research

Investigation of Soil and Vegetation Characteristics in Discontinuous Permafrost Landscapes Near Fairbanks, Alaska

Jacob F. Berkowitz, Christopher A. Hiemstra, and
Thomas A. Douglas

August 2015

Investigation of Soil and Vegetation Characteristics in Discontinuous Permafrost Landscapes Near Fairbanks, Alaska

Jacob F. Berkowitz

U.S. Army Engineer Research and Development Center (ERDC)
Environmental Laboratory (EL)
3909 Halls Ferry Road
Vicksburg, MS 39180

Christopher A. Hiemstra and Thomas A. Douglas

U.S. Army Engineer Research and Development Center (ERDC)
Cold Regions Research and Engineering Laboratory (CRREL)
Alaska Projects Office
Building 4070, 9th Street
Fort Wainwright, AK 99703

Final Report

Abstract

Alaska contains large areas of discontinuous permafrost, yet few studies examine the impact of microtopography on ground conditions and permafrost stability. This report uses vegetation and soil measurements to identify statistically significant differences to potentially classify permafrost ground-state conditions. The study identified significant relationships between soil parameters and vegetative community structure, including thicker peat layers in high microtopographic positions, greater active-layer thaw depths in high microtopographic positions, increased redox potentials in elevated microtopographic positions, and decreased soil moisture in higher topographic locations. Additionally, soil carbon and nitrogen concentrations increased in low microtopographic positions. These results suggest that soil and vegetation conditions may provide useful proxy measures in identifying permafrost and ground-ice features when incorporated into an integrated approach that combines belowground geophysics with aboveground remotely sensed terrain characteristics. Additional research is needed to combine soil and vegetation characteristics with sub-orbital and satellite-based remotely sensed measurements, such as airborne LiDAR, spectral reflectance, and high-resolution ground-level subsidence measurements.

Contents

Illustrations

Figures

Preface

This study was conducted for the Engineer Research and Development Center's Center-Directed Research Program under "Integrated Technologies for Delineating Permafrost and Ground-State Conditions." The project managers were David Ringelberg and Kevin Knuuti.

The work was performed by Dr. Jacob F. Berkowitz (Wetlands and Coastal Ecology Branch, Patty Tolley Tuminello, Chief), U.S. Army Engineer Research and Development Center, Environmental Laboratory (ERDC-EL), and Dr. Christopher A. Hiemstra (Terrestrial and Cryoshperic Sciences Branch, J. D. Horne, Chief) and Dr. Thomas A. Douglas (Biogeochemical Sciences Branch, Dr. Justin Berman, Chief), ERDC Cold Regions Research and Engineering Laboratory (CRREL). At the time of publication, Dr. Loren Wehmeyer was Chief of the Research and Engineering Division of ERDC-CRREL; and Kevin Knuuti was the Technical Director. The Deputy Director of ERDC-CRREL was Dr. Lance Hansen, and the Director was Dr. Robert Davis.

LTC John T. Tucker III was Acting Commander of ERDC; and Dr. Jeffery P. Holland was the Director.

Acronyms and Abbreviations

Ag	Silver
AgCl	Silver Chloride
C	Carbon
CF	Creamers Field
CH_4	Methane
CO_2	Carbon Dioxide
CRREL	Cold Regions Research and Engineering Laboratory
EL	Environmental Laboratory
ERDC	U.S. Army Engineer Research and Development Center
FAC	Facultative
FACU	Facultative Upland
FACW	Facultative Wetland
FL	ERDC Farmers Loop
GIS	Geographic Information System
HI	High
LO	Low
LiDAR	Light Detection and Ranging
N	Nitrogen
NRCS	Natural Resources Conservation Service
OBL	Obligate Wetland
Pt	Platinum
PT	ERDC Permafrost Tunnel
UPL	Obligate Upland
USACE	U.S. Army Corps of Engineers
USDA	U.S. Department of Agriculture
VWC	Volumetric Water Content

Unit Conversion Factors

Multiply	By	To Obtain
acres	4,046.873	square meters
inches	0.0254	meters

Executive Summary

The interior region of Alaska contains large areas of discontinuous permafrost, yet few studies examine the impact of microtopography on ground conditions and permafrost stability. This report uses vegetation and soil measurements to identify significant differences to potentially classify permafrost ground-state conditions.

We established three 400 m long research transects and identified statistically significant relationships between soil parameters and vegetative community structure. Peat layers were thicker in high microtopographic positions, decreasing at microtopographic lows (Mann Whitney $U = 46.0$; $p = 0.006$). Greater seasonally thawed active-layer depths were associated with high microtopographic positions with minimum active-layer thicknesses occurring in lower topographic locations ($U = 50.0$; $p = 0.009$). Higher redox potentials occurred in elevated microtopographic positions—ANOVA $F(1,28) = 7.80$; $p = 0.009$—and soil moisture increased in lower topographic locations—$F(1,27) = 5.07$; $p = 0.033$. We observed significantly higher soil carbon—$F(1,28) = 7.96$; $p = 0.009$—and nitrogen ($U = 51.5$; $p = 0.010$) concentrations in low microtopographic positions.

These results suggest that soil and vegetation conditions may provide useful proxy measures in identifying permafrost and ground-ice features when incorporated into an integrated approach that combines belowground geophysics with aboveground remotely sensed terrain characteristics. For example, areas exhibiting microtopographic features associated with polygonal ground are indicative of near-surface ice features and are easily distinguished with electrical resistivity tomography measurements. Additional research is needed to combine soil and vegetation characteristics with suborbital and satellite-based remotely sensed measurements, such as airborne LiDAR, spectral reflectance, and high-resolution ground-level subsidence measurements.

1　Introduction

Future climate scenarios predict a roughly 5°C increase in mean annual air temperatures for the Alaskan Interior over the next 80 years (Chapman and Walsh 2007). This will be enough to initiate permafrost degradation in many areas (Osterkamp and Jorgenson 2006; Marchenko et al. 2008) and is expected to lead to major changes in vegetation, biological and physical soil processes (Potter 2004; Walker et al. 2006; Wolken et al. 2011), and hydrology (Tarnocai and Campbell 2002; Davidson and Janssens 2006; Allison and Treseder 2011; Johnson et al. 2011; Sierra et al. 2011; Douglas et al. 2013, 2014). This will undoubtedly alter the soil thermal regime and is likely to cause subsidence and other ground-surface condition changes that could have major impacts on infrastructure design, operations, and maintenance. As such, tools are needed to help identify areas where permafrost thaw is a potential high risk for present and planned infrastructure.

We have been exploring how vegetation—its composition, diversity, and spectral signatures—may be associated with subsurface permafrost conditions. Our field sites are in the vicinity of Fairbanks in Interior Alaska (Figure 1). The Fairbanks area is underlain by discontinuous permafrost that ranges from a few meters to over 50 m thick and that most commonly underlies north-facing slopes, valley bottoms, and poorly drained soils (Jorgenson et al. 2001). The horizontal and vertical heterogeneity of permafrost distribution in the area prevents establishing any predictive capabilities for estimating the local, meter scale, permafrost extent. To address this, our sites were located in flat lowland terrain with little topography so that we could make measurements at a fine spatial scale (i.e., meters).

Many areas throughout the region exhibit complex microtopographic relief (Peterson and Billings 1980; Williams and Smith 1986; Engstrom 2005), and several studies investigate the effect of microtopography on frozen soil degradation (Jorgenson et al. 2006; Jorgenson and Osterkamp 2005). Zona et al. (2011) and others identified significant differences between soil characteristics (e.g., oxidation–reduction potential, active-layer depth, and moisture) related to soil stability. However, the majority of studies focused on ice-rich areas where near-surface-permafrost polygonal features

dominate microtopographic patterns (Figure 2). Few studies examine differences in soil characteristics related to microtopography in areas with discontinuous or deep permafrost.

Figure 1. A map of the Fairbanks area in Interior Alaska identifying the three study-site locations.

Figure 2. Ice wedge polygons along the Arctic Ocean Coast near Barrow, AK. The low-lying linear features are underlain by ice wedges; and the regions in between, also permafrost, are composed of frozen gravels, sands, and silts with an ice-rich matrix.

This document presents information on soil and vegetative site conditions along three 400–500 m long transects across landscapes underlain by discontinuous permafrost near Fairbanks, AK. The dataset provides information regarding the dominant vegetation along each transect and describes near-surface soil conditions within the seasonally thawed (active) layer. Study results indicate that several significant differences in microtopographic boundary conditions exist, and these can be characterized by unique soil and vegetation conditions. As such, our preliminary results suggest that there is potential in developing standoff detection techniques that capitalize on soil and vegetation signals to delineate permafrost regions. With further refinement and development, these standoff measurements have promise in identifying ground-ice features in the subsurface.

Department of Defense installations in Interior Alaska (e.g., Fort Wainwright, Fort Greely, Eielson Air Force Base, and Alaska Air National Guard) conduct training operations within a land area of more than 1.5 million acres that is underlain by discontinuous permafrost. This permafrost is close to thaw instability because the mean annual temperatures in the area are –1°C. Soil, moisture content, vegetation, and snow all play a role in the permafrost thermal regime; so mean annual temperature is not the only predictor of permafrost stability and instability. For example, Jorgenson et al. (2010) found permafrost to be stable at 2°C. Landscape disturbances can greatly affect surface soil, vegetation, and hydrology and can lead to permafrost degradation. The region has warmed 3°C since the 1960s and, as previously mentioned, is expected to warm another 5°C by 2100. This climate warming is expected to result in permafrost instability and will likely lead to more rapid and more severe responses to disturbance. The most common disturbances that impact permafrost stability include wildfire (Yoshikawa et al. 2003), recreational activities (e.g., airboat usage) (Racine et al. 1998), removing insulating soil layers, establishing roads and trails, and the creation of fire breaks (Fischer et al. 2013). Permafrost disturbances also impact carbon (C) cycling. Northern regions contain vast reservoirs of C; and with warming and permafrost thaw, the potential for emission as carbon dioxide (CO_2) and methane (CH_4) increases (Schuur et al. 2008; Lipson et al. 2012). Our ability to predict where, when, and how permafrost thaw will respond to local climatic, ecosystem, and hydrogeologic change is extremely limited; and identifying permafrost stability or instability and associated ground-ice features re-

mains a major objective for military installations, municipalities, local communities, industry, and the public. Because much of the land area in Interior Alaska is inaccessible by road, there is great need for geospatial tools that can remotely assess ground-state conditions.

Several studies have applied aerial imagery and remote-sensing applications toward identifying landscape features, including mapping permafrost and identifying ground-ice features (Etzelmüller et al. 2001; Kääb 2008). Additionally, several studies have investigated relationships between permafrost, ground conditions, and vegetation in northern regions (Jorgenson et al. 2001). For example, Stow et al. (2004) and others examined landscape and vegetation changes in the Arctic. However, most of the available literature focuses on the northern Arctic or on high-elevation areas where permafrost is continuous. Few studies apply these concepts to the discontinuous permafrost zone. A paucity of data exists regarding the relationship between soils and vegetation measurements and small-scale landscape features (e.g., microtopography) associated with permafrost and ground-ice features. To address this, the present study examines soil and vegetation characteristics within the discontinuous permafrost zone and has an end goal of supporting integrated approaches to delineate permafrost and ground-ice conditions.

2   Study Location and Field Sites

Field measurements occurred 15–19 July 2013 and 20–25 July 2014 along three 400–500 m research transects located at Creamers Field (CF), the Engineer Research and Development Center (ERDC) Permafrost Tunnel (PT), and the ERDC Farmers Loop (FL) research sites (Figure 1). All sample locations were in the vicinity of Fairbanks, AK. Zona et al. (2011) implemented a similar transect approach when investigating soil characteristics and microtopography in northern Alaska. The current study conducted vegetation surveys and aerial coverage estimates at 100 m intervals within each transect to determine dominant plants. Dominant species were selected using the 50/20 Rule (U.S. Army Corps of Engineers [USACE] 2007). Plant communities were also evaluated for hydrophytic status by using the Dominance Test (USACE 2007; Lichvar et al. 2014). The current report uses common names, but the appendices contain scientific names, references, and wetland plant indicator ratings. The appendices also include a full list of all plants observed at each sample location.

To investigate the impact of microtopography on soil conditions, we completed soil descriptions and sample collections in two locations at each 100 m interval along each transect. At each transect interval, we identified soil sampling areas in adjacent high (HI) and low (LO) topographic locations (Figure 3).

Soil sampling occurred at locations where HI and LO microtopographic positions were co-located within one linear meter of one another. As a consequence of the close proximity, all of our paired sites experience the same climate conditions. We applied this approach so that we could identify whether microtopographic differences in the landscape were associated with unique soil characteristics.

Soil measurements included soil horizon depth, color, redoximorphic features, and texture. We determined soil moisture in the field by using five repeated measurements with a Spectrum Field Scout TDR 200 Soil Moisture Probe. We collected soil samples for bulk density and volumetric water content (VWC). Our study determined the soil total C and nitrogen (N) concentrations via combustion by using an Elementar Vario Macro Carbon

Nitrogen analyzer (900°C) (Kahn 1988; Klute 1986). To compare across transects and sample locations, we calculated the amount of soil C and N occurring in the upper 20 cm of the soil surface. This represents the area considered critical for soil biogeochemical functioning due to high concentrations of organic matter and soil microbes (Chorover et al. 2007; Segers 1998).

Figure 3. The sample layout displaying microtopographic high (HI) and low (LO) sample locations at the ERDC Farmers Loop Experimental Station. Note that adjacent sample locations are within one linear meter of each other.
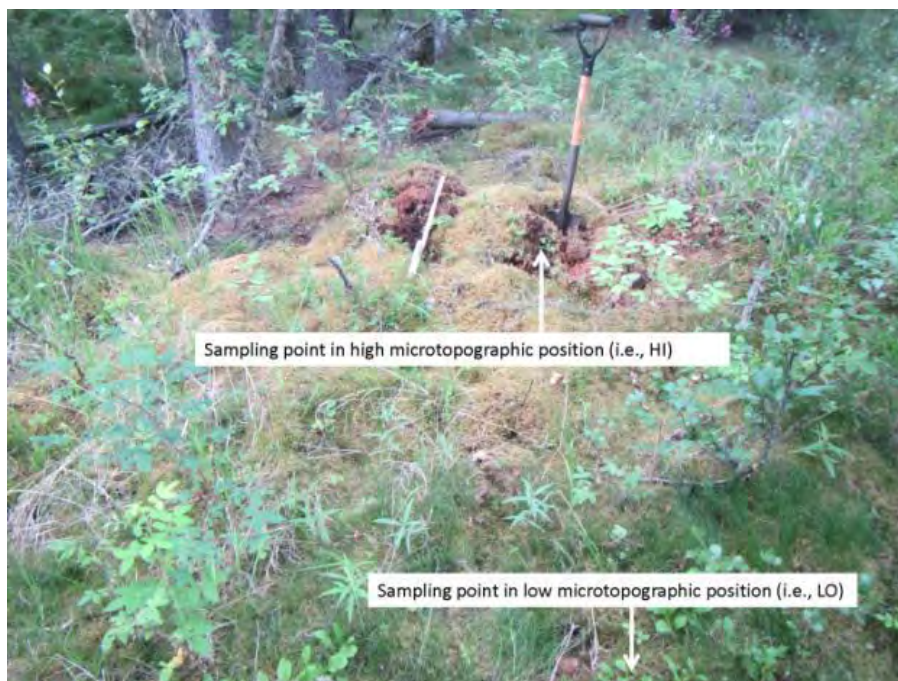
We selected paired HI and LO topographic positions for redox measurements (Figure 4) and recorded them 5 cm below the first mineral soil horizon or at a depth of 20 cm if no mineral soil was present. All redox measurements, 5 replicates at each location, used Ag/AgCl (silver/silver chloride) reference electrodes (Vepraskas and Faulkner 2001); and results underwent corrections for reference electrode potential. Each platinum (Pt) electrode was calibrated in buffered quinhydrone solution (Sparks et al. 1996). All soils were considered chemically reduced when the corrected redox value occurred below the level depicted on the Eh-pH curves outlined in Reddy and DeLaune (2008) and Faulkner et al. (1989). Statistical analysis used linear regression and either (1) ANOVA or (2) the non-parametric Mann-Whitney U test based on the results of data normality

testing (Shapiro-Wilk); all significance was determined at the $\alpha = 0.05$ level (IBM Corp. 2011).

Figure 4. An example of an oxidation–reduction potential sample scheme displaying replicate Pt electrodes. Note that adjacent HI and LO sample locations are within 1 m of each other.

3   Results

The following section provides information on the dominant plant species and soil characteristics observed along each research transect.

3.1   Creamers Field (CF)

The CF transect spanned 500 linear m with samples located at CF-0, CF-100, CF-200, CF-300, CF-400, and CF-500, where each number corresponds to the distance in meters along the transect (Figure 5). This was a lowland site with an overall elevation across the transect remaining approximately flat at 137 m above sea level. However, localized micro-elevation changes were abundant throughout the area, including patches of polygonal ground, drainage pathways, sunken forests, and tussock zones, which combined created a complex microtopographic relief of up to 2 m. Within CF-0, a mixed tree strata was dominated by paper birch (*Betula neoalaskana*) and alder (*Alnus rubra*) with alder dominating the sapling shrub layer and prickly rose dominating the herbaceous layer (Figure 6). Fireweed (*Chamerion angustifolium*), salmonberry (*Rubus* spp.), and sphagnum moss were also common in the understory; but they were not the dominant species. Soils consisted of dark, fibrous peats in the upper layer followed by mucky peats in lower layers. The HI sampling location also contained some loamy clay materials displaying signs of biogeochemical reduction, resulting in the formation of redoximorphic depletions (10%) and iron and manganese concentrations (5%). All soils at CF-0 met hydric soil indicator A1 Histosol (Figure 6).

CF-100 exhibited similar forest-cover values with the addition of black spruce in the sapling strata and increased sphagnum ground cover. Soils were similar to those observed at CF-0 although the depth to permafrost was reduced in both LO and HI sampling locations. All soils at CF-100 met hydric soil indicator A1 Histosol and/or A2 Histic epipedon. Moving towards CF-200 resulted in a decrease in tree canopy cover (15% total cover) and the inclusion of willows in the sapling strata. Additionally, salmonberry and tussock cottongrass began to dominate the herbaceous layer. Soils consisted of dark peat underlain by mucky peat with active-layer depths increasing in both LO and HI sampling positions. All soils at CF-200 met hydric soil indicator A1 Histosol and/or A2 Histic epipedon.

Tree cover continued to decrease in CF-300 (5%), accompanied by the inclusion of dwarf birch (*Betula nana*) in the understory. The herbaceous layer remained dominated by sphagnum, salmonberry, and tussock cottongrass (*Equisetum angustifolium*). Soils at CF-300 consisted of a single homogenous layer of dark muck (i.e., sapric material) in the LO sampling position and dark peat in the HI sampling position. All soils at CF-300 met hydric soil indicator A1 Histosol and/or A2 Histic epipedon.

CF-400 and CF-500 displayed similar plant communities with no tree canopy cover, a sapling and shrub strata dominated by willow (*Salix* spp.) and dwarf birch, and tussock cottongrass in the herb layer. Soils in LO sampling positions exhibited dark layers of peat and muck. No HI samples were collected at CF-400 and CF-500 due to difficulty in identifying polygons in the tussock landscape. All soils at CF-400 and CF-500 met hydric soil indicator A1 Histosol.

Figure 5. A May 2014 airborne LiDAR image with yellow symbols denoting the Creamers Field sampling locations. Note the presence of pattered ground (ice wedge polygons) throughout the transect, but the thick forest vegetation from 0 to 100 m makes it more difficult to discern.
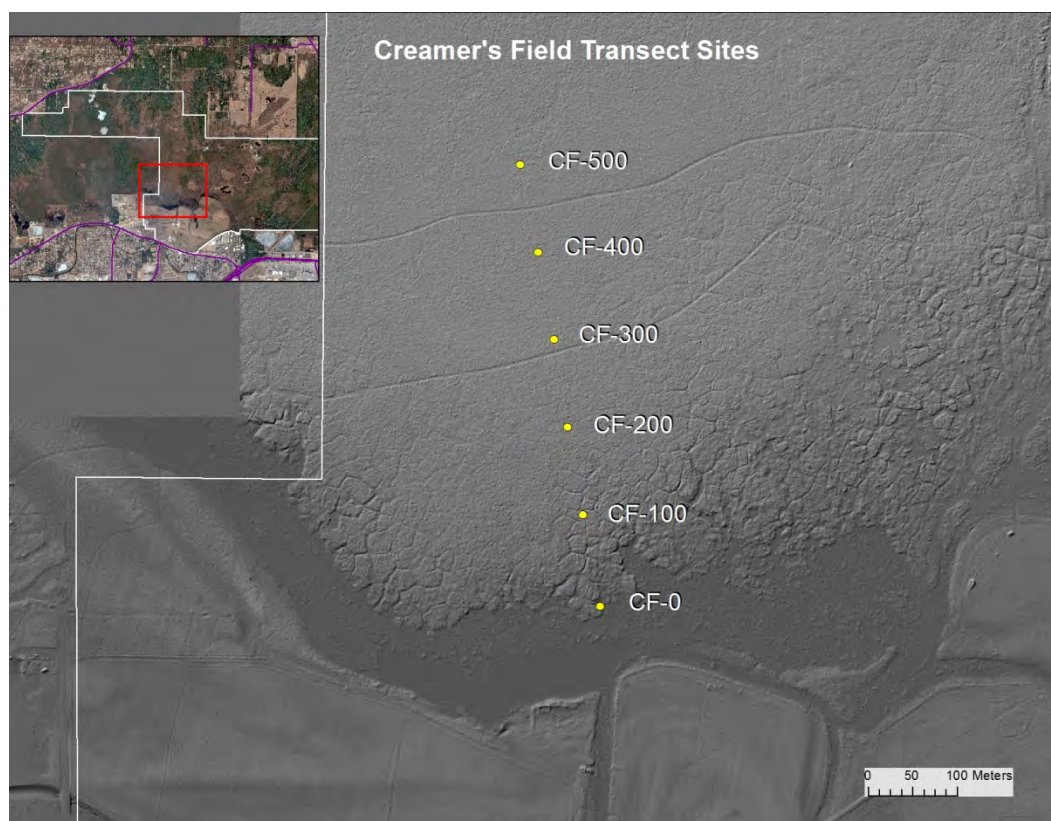
Figure 6. A visual representation of CF research transect results. Dominant vegetation species are reported for tree (*1*), sampling/shrub (*2*), and herbaceous (*3*) strata. Soil profiles report data were collected in HI and LO locations. Volumetric water content (VWC) values are based on laboratory data. Note that active-layer depth (i.e., the extent of the soil pit depth) remains deeper in HI sampling positions. Additionally, the depth of all peat layers is deeper in HI sampling positions. VWC increases both with depth and linearly across the transect.

1. P. Birch/Alder
2. Alder
3. Prickly Rose
CF-0

1. P. Birch
2. B. Spruce/Alder
3. Sphagnum
CF-100

1. P. Birch/B. Spruce
2. Alder/Willow/
P. Birch/B. Spruce
3. Salmonberry/
Tussock cottongrass
CF-200

1. B. Spruce
2. Willow/P. Birch/Dwarf
Birch
3. Salmonberry/ Tussock
Cottongrass/ Sphagnum
CF-300

1. None
2 . Willow/Dwarf Birch
3. Tussock Cottongrass
CF-400 and CF-500

137 m elevation

137 m

HI

0-11.5 cm 7.5YR 3/2 Peat 60% fibers; 8% VWC

11.5-23 cm 2.5Y 4/4 Fine silt 10% 10YR 5/1 depletions; 5% 10YR 4/4 concentrations; wavy boundary; 13% VWC

23-64 cm 7.5YR 4/3 Mucky peat 20% fibers; 17% VWC

LO

0-7.6 cm 7.5YR 3/2 Peat 70% fibers; 6% VWC

7.5-30 cm 7.5YR 3/3 Mucky peat 40% fibers; 18% VWC

30-48 cm 7.5YR 3/3 Mucky peat 25% fibers; 24% VWC

LO

0-15 cm 7.5YR 3/2 Peat 80% fibers; 52% VWC

HI

0-18.5 cm 7.5YR 3/2 Peat 60% fibers; 4% VWC

18-30 cm 7.5Y 2.5/2 Mucky modified silt loam; 10 YR 4/2 depletions 10%; 7.5YR 5/4 concentrations; 29% VWC

LO

0-5 cm 7.5YR 3/2 Peat 70% fibers; 54% VWC

5-30 cm 7.5YR 3/2 Mucky peat 60% fibers; 68% VWC

HI

0-25 cm 7.5YR 2.5/1 Peat 80% fibers; 18% VWC

25-38 cm 2.5Y 2.5/2 Muck 10% fibers; 57% VWC

LO

0-23 cm 7.5YR 3/2 Muck 20% fibers; 60% VWC

HI

0-30 cm 7.5YR 3/3 Peat 80% fibers; 47% VWC

LO

0-25 cm 7.5YR 2.5/1 Peat 60% fibers; 44% VWC

LO

0-25 cm 7.5YR 2.5/1 Muck 20% fibers; 68% VWC

Soil C concentrations across the transect sampling points ranged from 6.0 to 16 kg, while soil N ranged from 0.1 to 0.9 kg in near-surface layers (i.e., upper 20 cm; Figure 7). In general, transect soil nutrient concentrations in LO sampling positions remained elevated compared to HI microtopographic positions. Soils within the CF transect exhibited both oxidized and reduced conditions; and in general, chemical reduction was greater in LO sampling positions. However, two of the four HI sampling positions were also chemically reduced, compared to four out of five in LO microtopographic positions.

Vegetation shifted significantly across the CF transect; highly forested area converted to open tussock meadow (Figure 8). Additionally, soil VWC increased both with soil depth and across the CF transect. Surface-soil layers at CF-0 were below 20% VWC while surface soils at CF-400 and CF-500 contained more than 40% VWC. Other trends identified within the transect include relationships between permafrost and peat depth in relation to LO and HI sampling positions. In all cases, HI sample points exhibited deeper active-layer thaw depths and thicker peat layers.

Figure 7. CF research transect (*A*) near-surface soil C, (*B*) N concentrations, and (*C*) soil oxidation–reduction-potential results; note that the sampling locations occurring below the line were chemically reduced during data collection.
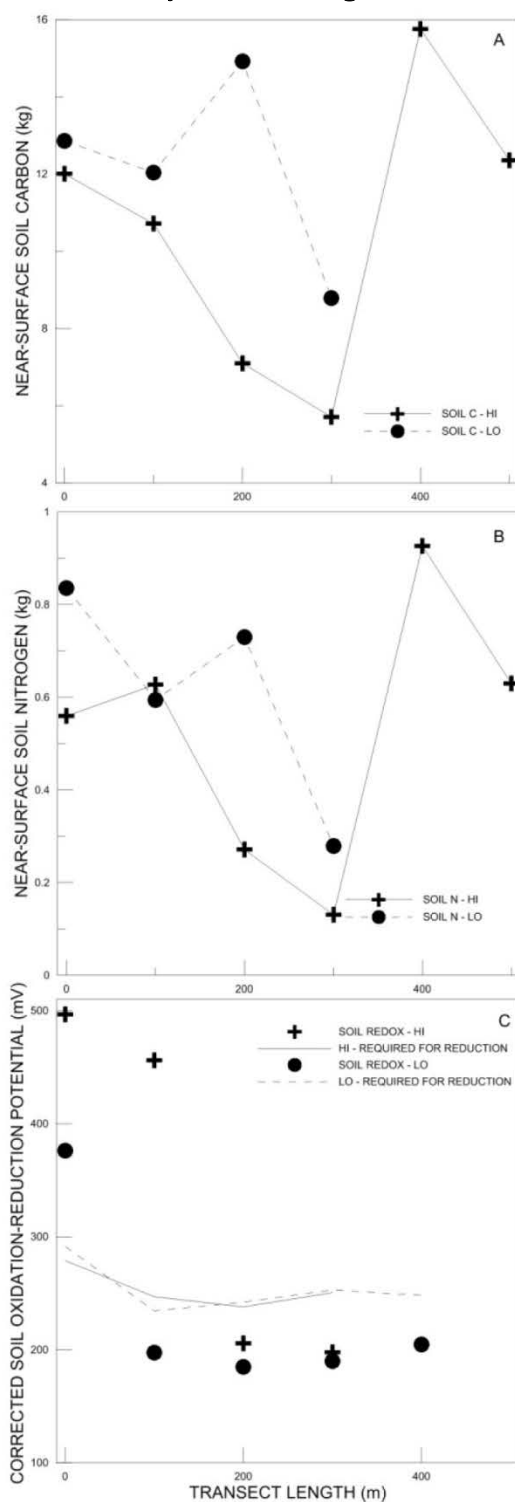
Figure 8. CF research transect (*A*) tree cover, (*B*) average soil moisture (VWC), (*C*) peat layer depth, and (*D*) active-layer depth within LO and HI sampling positions across the research transect. Note that the active layer (i.e., the extent of the soil pits) remains deeper in HI sampling positions. Additionally, the depth of all peat layers is deeper in HI sampling positions. VWC increased linearly across the transect as tree canopy declined.
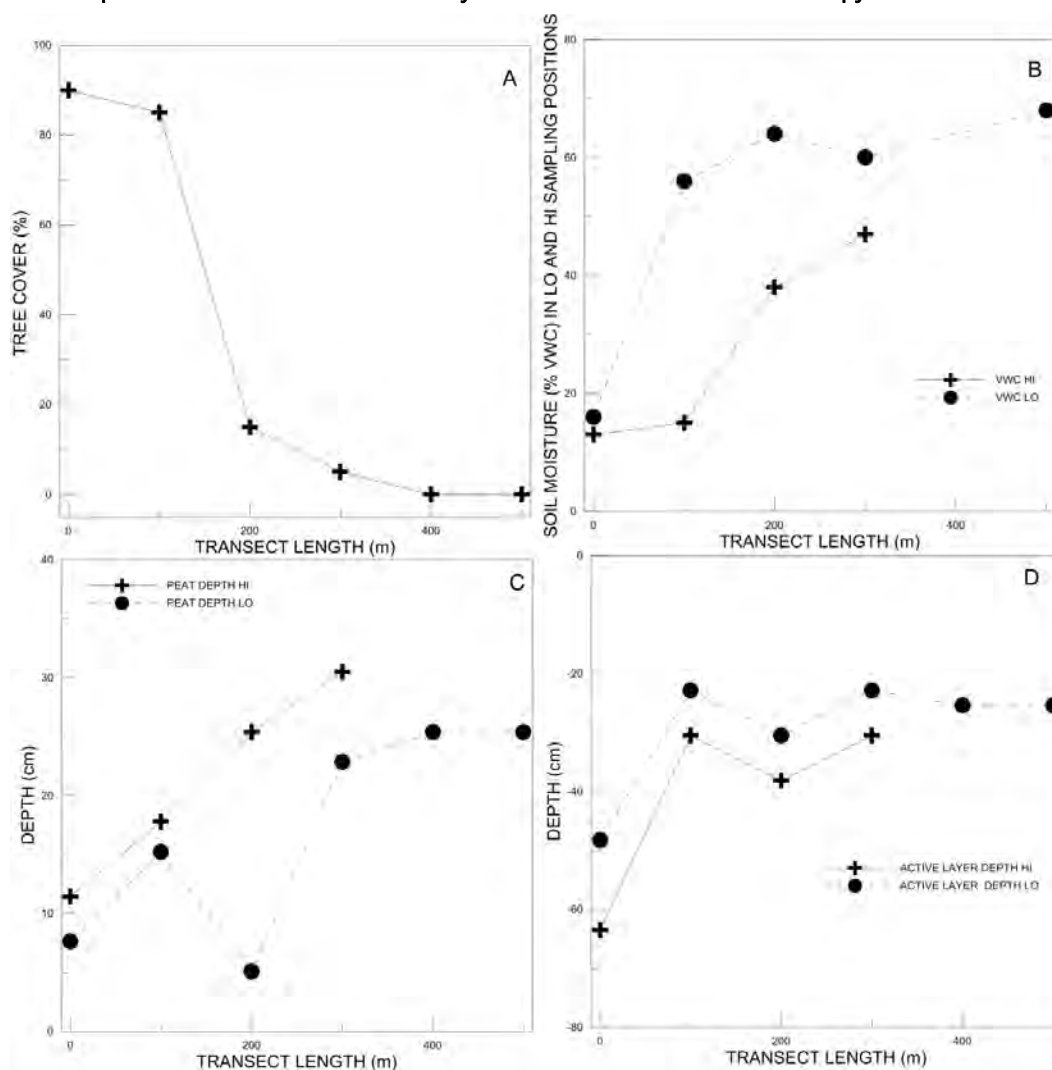
3.2 Farmers Loop (FL)

The FL transect spanned 400 m of lowlands with samples located at FL-0, FL-100, FL-200, FL-300, and FL-400, corresponding to the distance in meters along the transect (Figure 9). The overall elevation decreased slightly across the transect from approximately 143 to 137 m (FL-0 to FL-400). Along the FL transect, local micro-elevation changes were associated with patches of polygonal ground, drainage pathways, and tussocks. Within FL-0, a mixed tree strata (20% cover) was dominated by black spruce, with black spruce and paper birch composing the sapling and

shrub layer (Figure 10). Dwarf birch, coltsfoot (*Tussilago farfara*), and bluejoint reedgrass (*Calamagrostis canadensis*) dominated the herbaceous layer. Fireweed, sphagnum, watermelon berry, wild strawberry, blueberry (*Vaccinium alaskaense*), sedge (*Carex* spp.), salmonberry (*Rubus* spp.), prickly rose (*Rosa acicularis*), meadow horsetail (*Equisetum pratense*), and other herbaceous plants were present along the transect but not dominant at FL-0. Soils consisted of dark, fibrous peats in the upper layer followed by high organic content loamy materials in the underlying layers. The lowest soil horizon examined consisted of gray depleted mineral matrixes with between 20% and 30% iron and manganese redoximorphic concentrations. The locations and depletions within this layer indicated long-term saturation and water-table fluctuations in the range of 10–20 cm in both LO and HI sampling positions. All soils at FL-0 met hydric soil indicator Alaska redox with 2.5Y hue.

Figure 9. An image denoting the Farmers Loop research transect laid over a May 2014 LiDAR (Light Detection and Ranging) image. The yellow symbols represent surveying and sample collection locations whereby the number corresponds to the distance (in meters) across the transect.
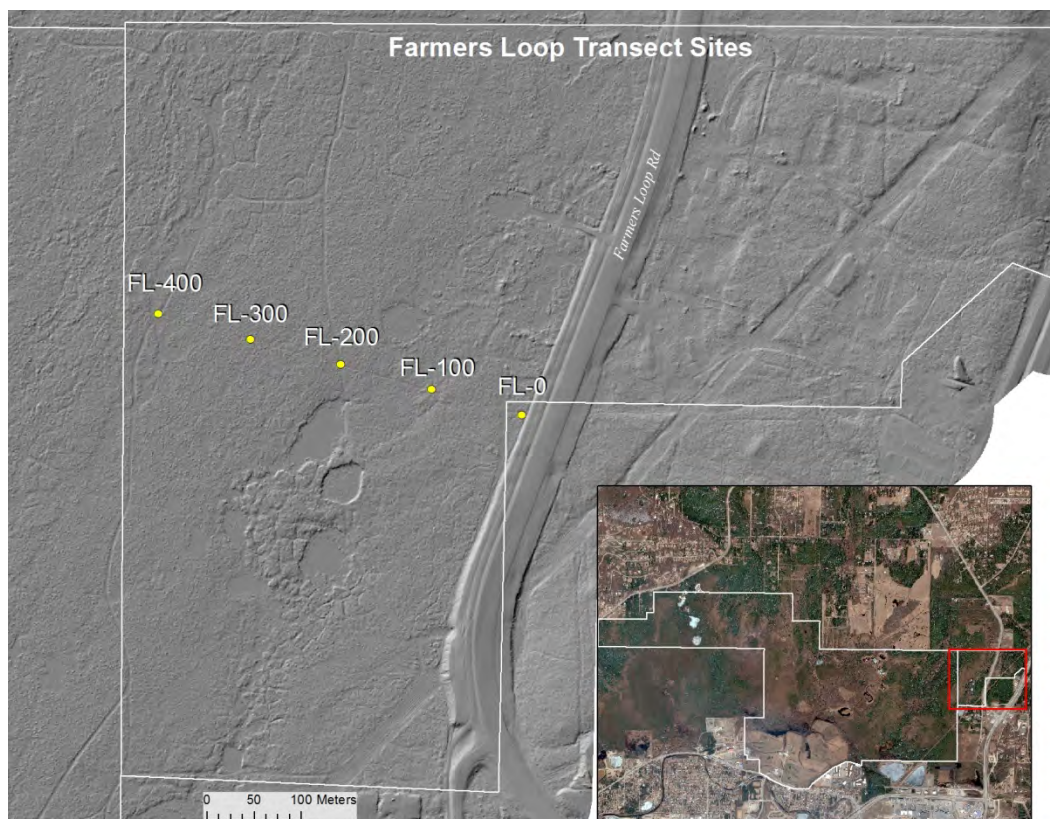
Figure 10. A visual representation of the FL research transect results. Dominant vegetation species are reported for tree (*1*), sampling/shrub (*2*), and herbaceous (*3*) strata. Soil profiles report data were collected in HI and LO locations. Volumetric water content (VWC) values are based on laboratory data. Note that active-layer depth (i.e., the extent of the soil pits) remains deeper in HI sampling positions. Additionally, the depth of peat layers is deeper in HI sampling positions. VWC increases both with depth and in areas displaying limited tree cover.
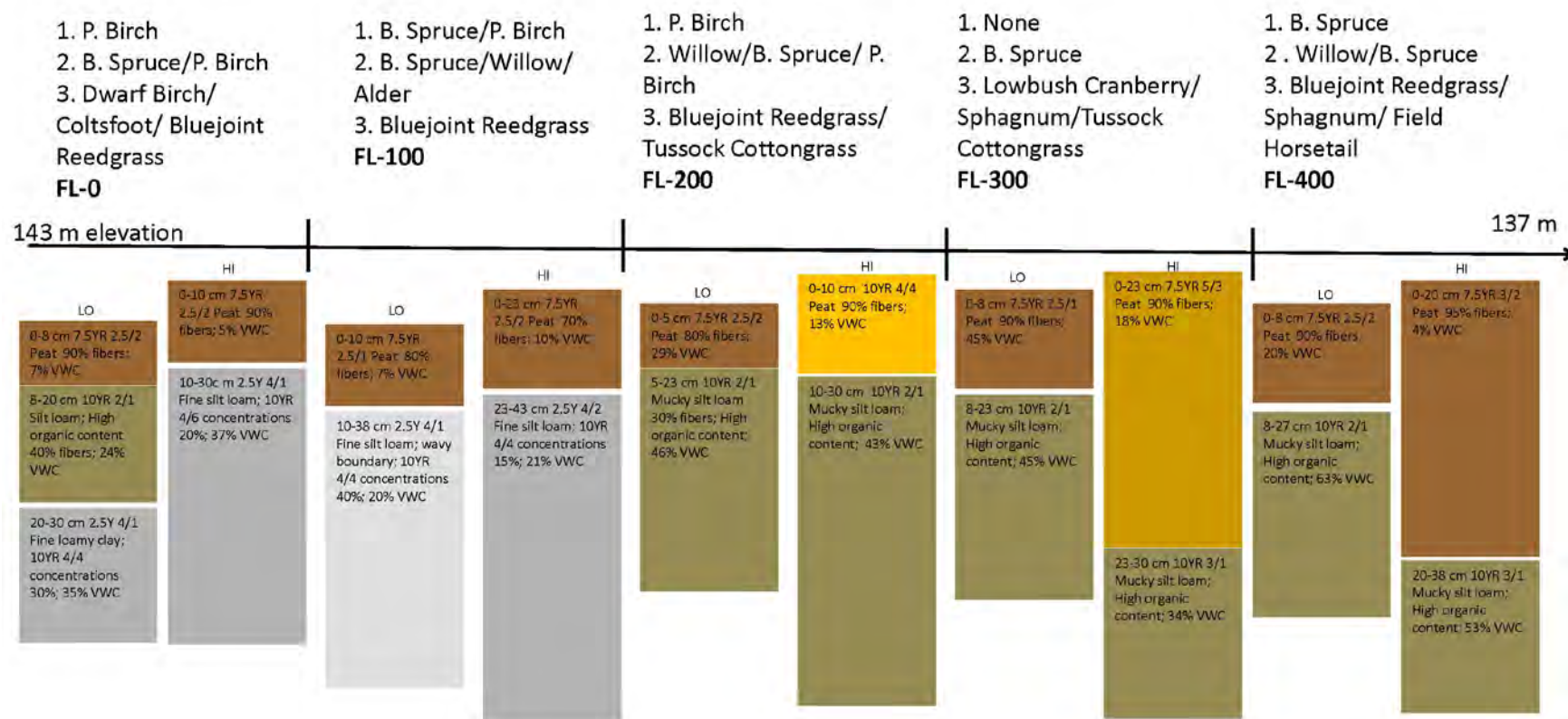
FL-100 displayed increased tree cover (40%) relative to FL-0, and the forest was dominated by paper birch and black spruce in the overstory with willow, black spruce, and alder abundant in the sapling strata (Figure 11A). Bluejoint reedgrass dominated the herbaceous layer. Soils displayed 20–23 cm of peat underlain by a depleted loamy clay matrix. The base of the active layer exhibited highly reducing conditions with gley and/or depleted matrix colors and 15%–40% redoximorphic concentrations (Figure 11B). The active-layer depth was higher in both the LO and HI sampling locations as compared to FL-0. Hydric soil indicators Alaska redox with 2.5Y hue occurred in both HI and LO sample locations.

Figure 11. (*A*) The vegetation present at FL-100. (*B*) Soil profiles described at FL-100 with the HI sampling position (*left*) and LO sampling position (*right*). Note the increased depth of dark peat material within the HI sample position. Scale is in inches.
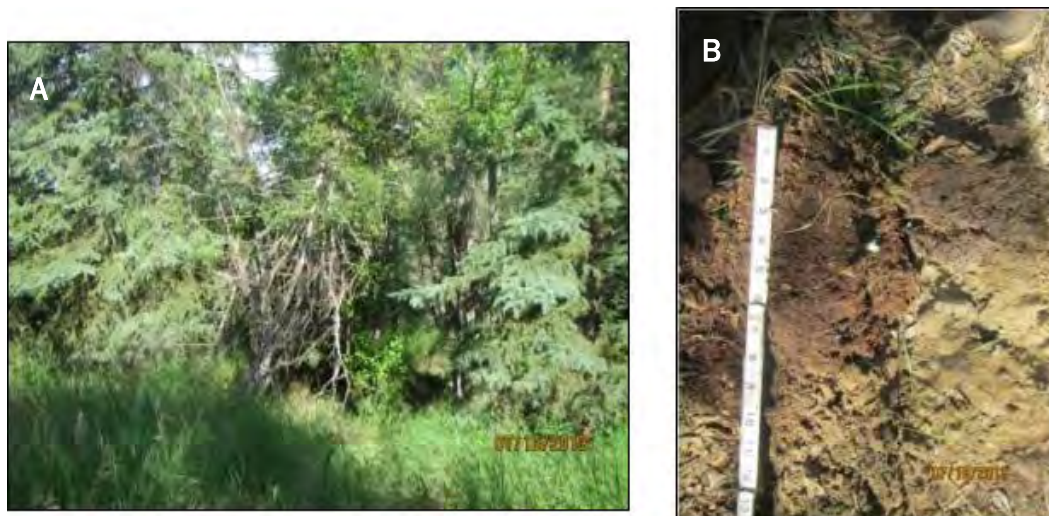
Moving towards FL-200 resulted in a decrease to only 5% cover (paper birch) in the tree strata with willow, paper birch, and black spruce dominating the sapling strata. Bluejoint reedgrass and tussock cottongrass dominated the herbaceous layer. Soils consisted of peat underlain by dark, mucky modified silt loams, indicating extended periods of soil saturation within 5–13 cm of the surface. Active-layer depths were shallower than observed at FL-100.

FL-300 lacked tree cover and had a sapling strata dominated by black spruce. The herbaceous layer remained dominated by tussock cottongrass, lowbush cranberry (*Viburnum trilobum*), and sphagnum moss (Figure 12A). Soils at FL-300 consisted of a fibrous peat underlain by dark, mucky

modified silt loams. Hydric soil indicator Histic epipedon was met at FL-300 (Figure 12B).

Figure 12. (*A*) A landscape view of FL-300, which lacks a tree strata layer. (*B*) Soil profiles of HI (*left*) and LO (*right*) sample positions. Note that the peat layer remains thicker within the HI sample location. Scale is in inches.
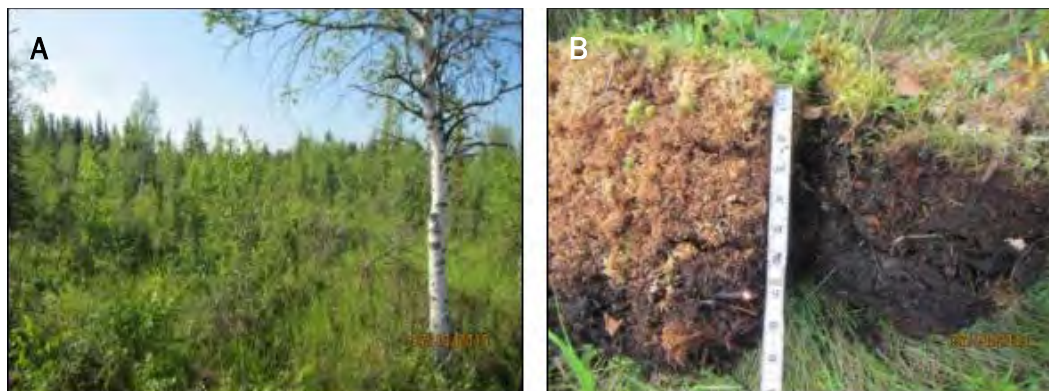
The plant community surrounding FL-400 displayed black spruce trees (30% cover), willow and black spruce saplings, and a herbaceous layer dominated by bluejoint reedgrass, field horsetail (*Equisetum arvense*), and sphagnum moss. Soils at FL-400 contained dark-brown peats underlain by dark, mucky modified mineral horizons.

Soil C concentrations along the FL transect ranged from 2.2 to 14 kg while soil N ranged from 0.03 to 0.68 kg in near-surface layers (Figure 13). Both soil C and N concentrations in LO sampling positions remained elevated when compared to HI microtopographic positions. Soils within the FL transect exhibited both oxidized and reduced conditions. In general, soil oxidation–reduction potentials were lower in LO sampling positions. One of the five HI sampling positions were chemically reduced compared to four out of five in LO microtopographic positions.

Vegetation shifted across the FL transect from 20% to 40% forested areas at FL-0 and FL-100; converting to lower cover, open areas at FL-200 and FL-300 (less than 5% cover); and shifting to 40% forest cover at FL-400 (Figure 14). Soil VWC increased with reduced canopy cover. As seen in the CF transect data, we identified in FL relationships between active-layer and peat depth in relation to LO and HI sampling positions. In all cases, HI sample points exhibited thicker active-layer and peat depths.

Figure 13. FL research transect (*A*) near-surface soil C, (*B*) N concentrations, and (*C*) soil oxidation–reduction potential results. Note that the sampling locations occurring below the line were chemically reduced during the data collection period.
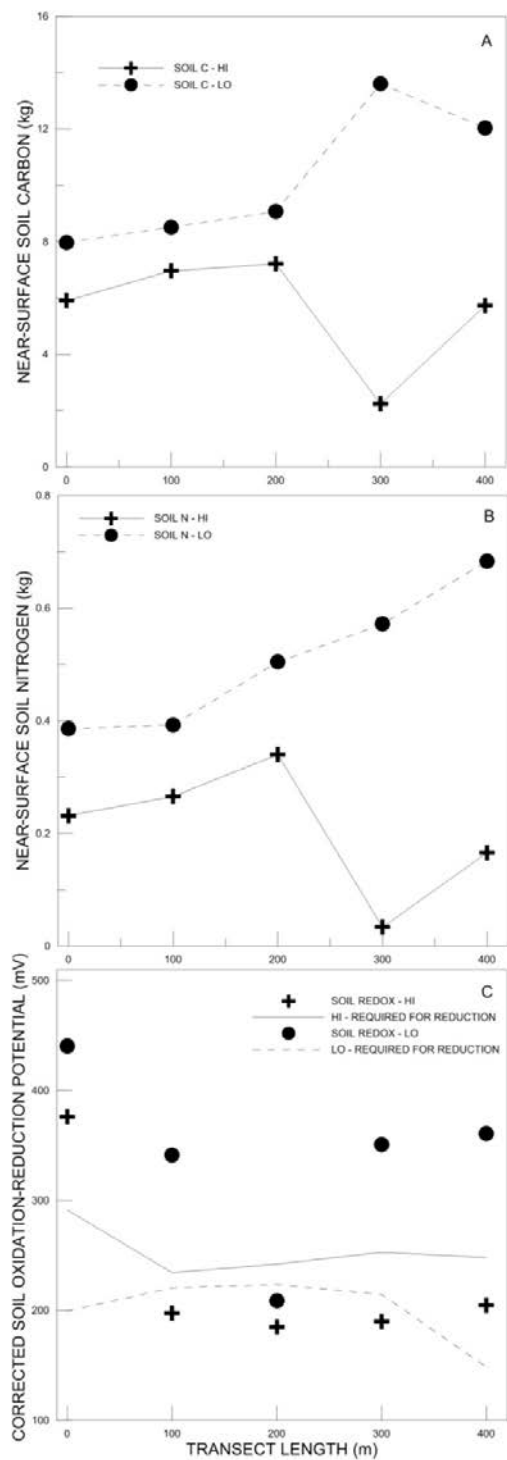
Figure 14. FL research transect (*A*) tree cover, (*B*) average soil moisture (VWC), (*C*) peat layer depth, and (*D*) active-layer depth within LO and HI sampling positions across the research transect. Note that active-layer depth (i.e., the extent of the soil pits) remains deeper in HI sampling positions. Additionally, the depth of all peat layers is thicker in HI sampling positions. VWC generally increases both with depth and in areas lacking tree canopy cover.
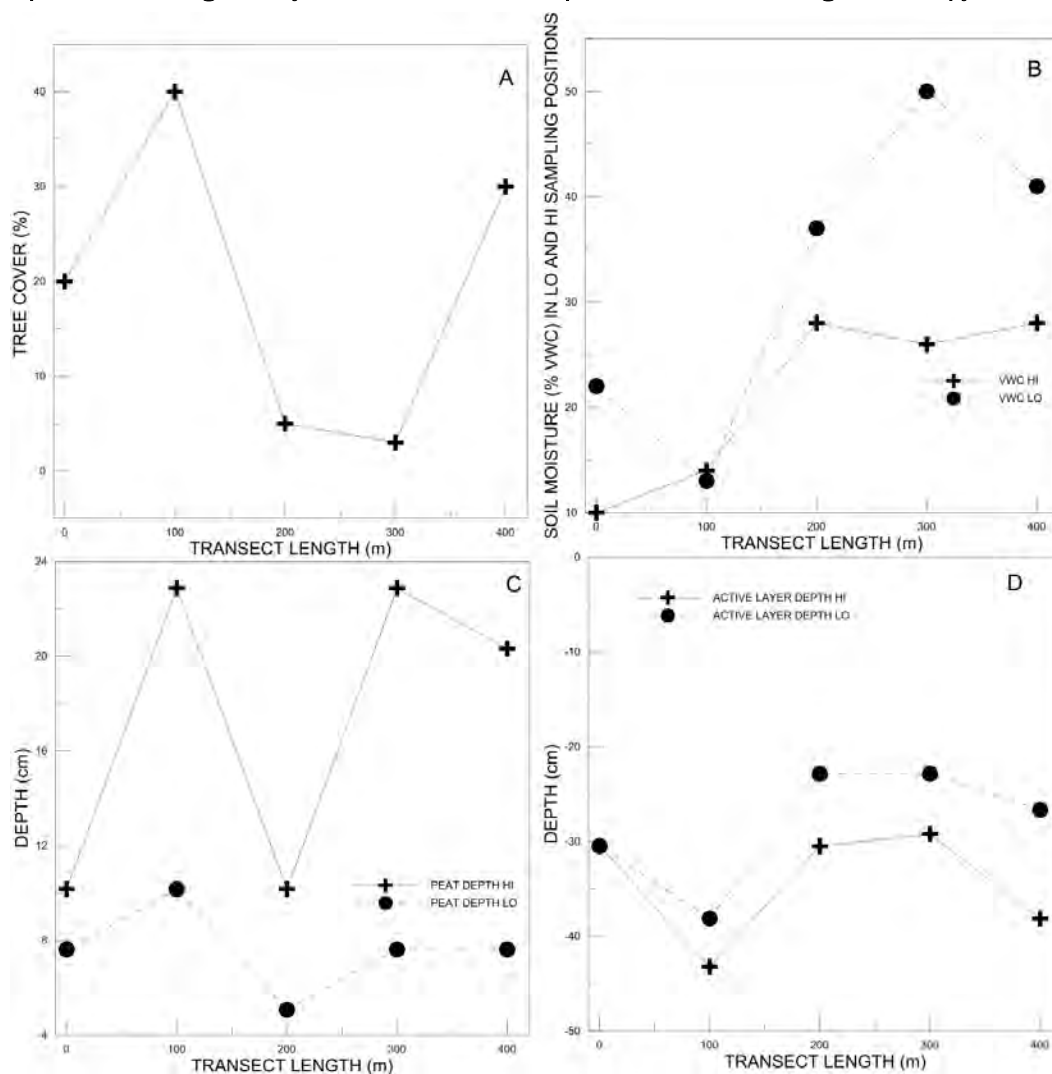
3.3 Permafrost Tunnel (PT)

The PT transect spanned 400 m across upland boreal forest with samples located at PT-0, PT-100, PT-200, PT-300, and PT-400, corresponding to the distance in meters along the transect (Figure 15). The overall elevation across the transect rose steadily from approximately 237 to 256 m (PT-0 to PT-400). As seen at the CF and FL transects, local elevation changes re-

mained abundant throughout the area with patches of polygonal ground, drainage pathways, and tussocks creating complex microtopographic relief. Within PT-0, a mixed tree strata (50% cover) was dominated by black spruce and aspen (*Populus tremuloides*) with black spruce dominating the sapling shrub layer. Labrador tea (*Rhododendron groenlandicum*), dwarf birch, and sphagnum moss dominated the herbaceous layer (Figure 16). Coltsfoot, salmonberry, blueberry, and bluejoint reed grass were also observed in the area but were not dominant species. Soils consisted of dark, fibrous peats in the upper layer followed by high organic content loamy materials in the underlying layers. The lower extent of the active layer consisted of gray depleted matrixes with between 20% and 30% iron and manganese redoximorphic concentrations. The redoximorphic features and depleted matrixes indicated long-term saturation and water-table fluctuations in the range of 18–25 cm in both LO and HI sampling positions. All soils at PT-0 met hydric soil indicator Alaska redox with 2.5Y hue.

Figure 15. The Permafrost Tunnel transect laid over a May 2014 LiDAR collection.
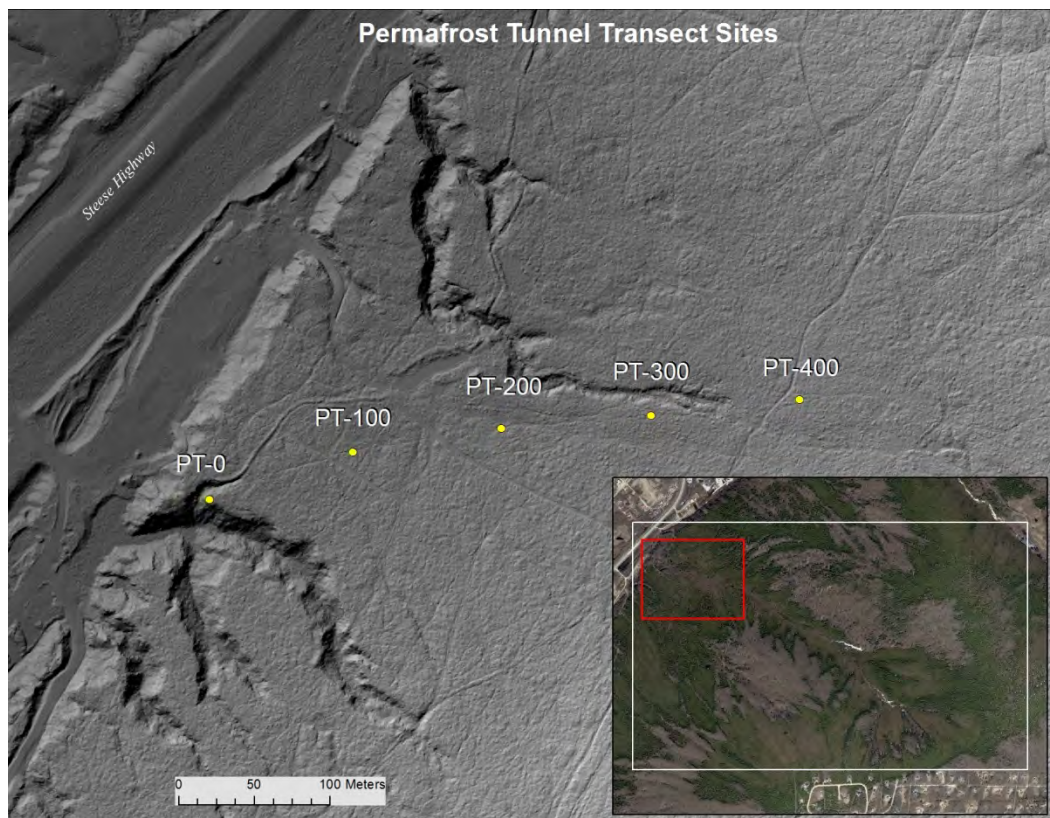
Figure 16. A visual representation of PT research transect results. Dominant vegetation species are reported for tree (*1*), sampling/shrub (*2*), and herbaceous (*3*) strata. Soil profiles report data were collected in HI and LO locations. Volumetric water content (VWC) values are based on laboratory data. Note that active-layer depth (i.e., the extent of the soil pits) remains deeper in HI sampling positions. Additionally, the depth of all peat layers is deeper in HI sampling positions. VWC increases both with depth and in areas displaying lower tree cover.
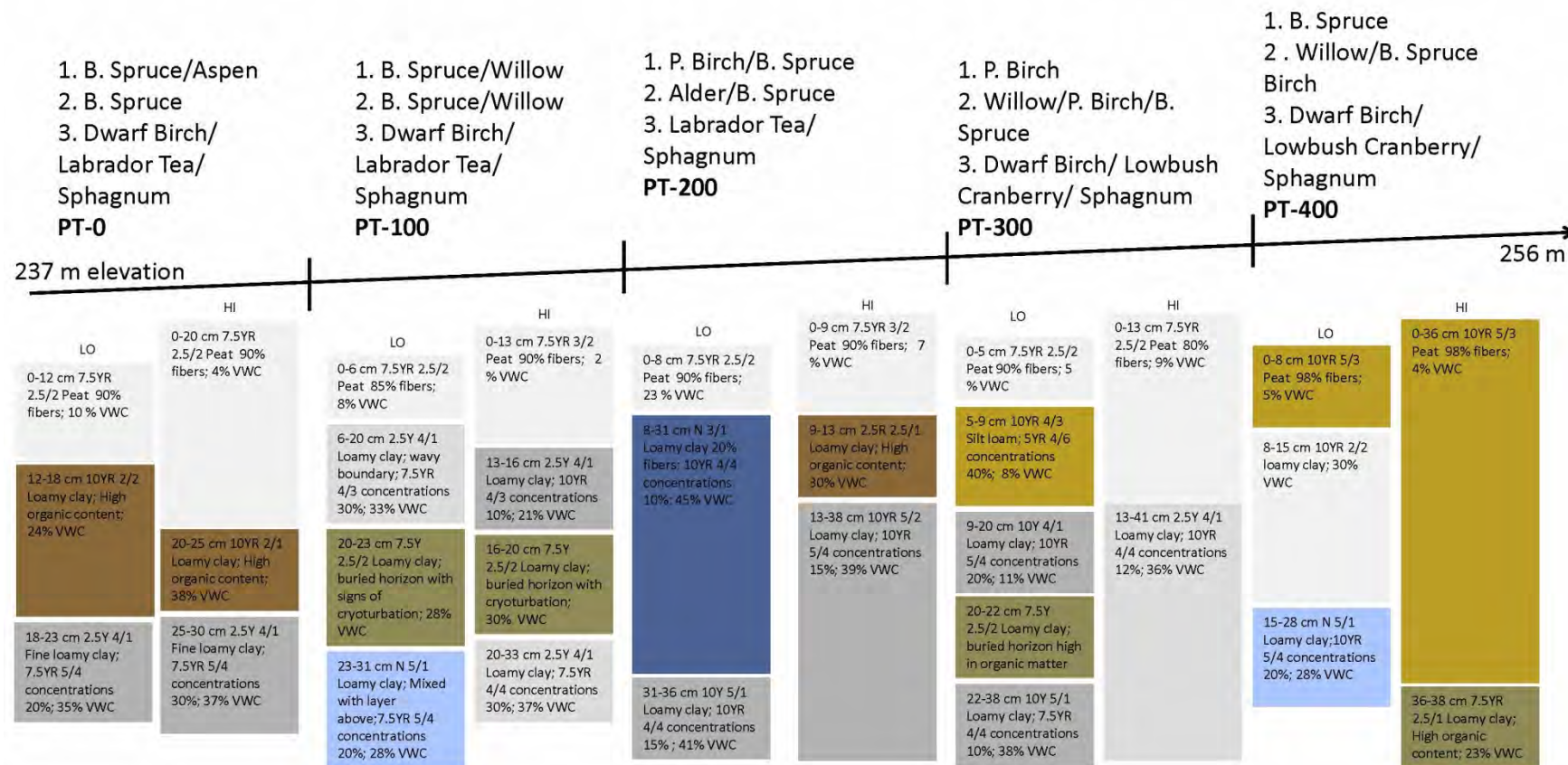
PT-100 displayed decreased forest cover (10%) and included willow in the sapling strata (Figure 16). Soils displayed 6–13 cm of peat underlain by a depleted loamy clay matrix. In both LO and HI sampling positions, a dark, high organic content mineral layer suggested the presence of a buried soil horizon (Figure 17). The base of the active layer exhibited highly reducing conditions with gley and/or depleted matrix colors and 20%–30% redoximorphic concentrations. The active-layer depth was higher in both LO and HI sampling locations as compared to PT-0. Hydric soil indicators were met in both LO (Alaska redox) and HI (Alaska redox with 2.5Y hue) sample locations.

Figure 17. A soil profile observed at PT-100 in the HI sampling position. Note the presence of a buried soil horizon. Scale is in inches.

Moving towards PT-200 resulted in an increase in tree canopy cover (15% total cover) dominated by paper birch and black spruce and the inclusion of alder in the sapling strata. The herbaceous layer remained dominated by Labrador tea and sphagnum moss. Soils consisted of dark peat underlain by gley or depleted mineral matrixes with active layers increasing in both LO and HI sampling positions compared to PT-100.

PT-300 continued to display limited tree cover (10% paper birch) accompanied by the inclusion of willow and black spruce in the sapling shrub strata. The herbaceous layer remained dominated by dwarf birch, lowbush cranberry, and sphagnum moss. Soils at PT-300 consisted of a dark peat (i.e., fibric material) underlain by depleted matrixes containing 10%–20% redoximorphic concentrations. The LO sampling location also exhibited a buried horizon. Hydric soil indicator Alaska redox with 2.5Y hue was met at PT-300.

The plant community surrounding PT-400 displayed black spruce trees (15% cover); willow and black spruce saplings; and a herbaceous layer dominated by dwarf birch, lowbush cranberry, and sphagnum moss (Figure 18A). Soils at PT-400 contained brown peat underlain by dark mineral horizons. The LO sampling position exhibited a gley matrix at depth and met hydric soil indicator Alaska gleyed without hue 5Y; the HI sampling position met hydric soil indicator A2 Histic epipedon (Figure 18C).

Soil C concentrations ranged from 2.0 to 6.9 kg, while soil N ranged from 0.03 to 0.33 kg in near-surface layers across the transect locations (Figure 19). Both soil C and N concentrations in LO sampling positions were elevated compared to corresponding HI microtopographic positions. Soils within the CF transect exhibited both oxidized and reduced conditions. Two of the five HI sampling positions were chemically reduced compared to four out of five in LO microtopographic positions.

We observed vegetation shifts across the PT transect as forested areas at PT-0 converted to open areas at PT-100 and then shifted to between 10% and 15% forest cover at the remainder of the transect sample points (Figure 20). Soil VWC generally increased with soil depth and in areas with reduced canopy cover. As seen in the CF and FL transect data, we identified relationships between permafrost and peat depth in relation to LO and HI sampling positions. In all cases HI sample points exhibited deeper permafrost and thicker peat layers (Figure 20).

Figure 18. (*A*) A landscape view of PT-400 exhibiting limited tree cover of black spruce. Willow and black spruce dominate the sapling/shrub strata while herbaceous species of dwarf birch, sphagnum moss, and lowbush cranberry dominate the lower strata. Soil samples examined in (*B*) HI and (*C*) LO landscape positions. Note the thicker peat layer and deeper active-layer depths associated with HI sampling position compared to the LO microtopographic position. Scale is in inches.
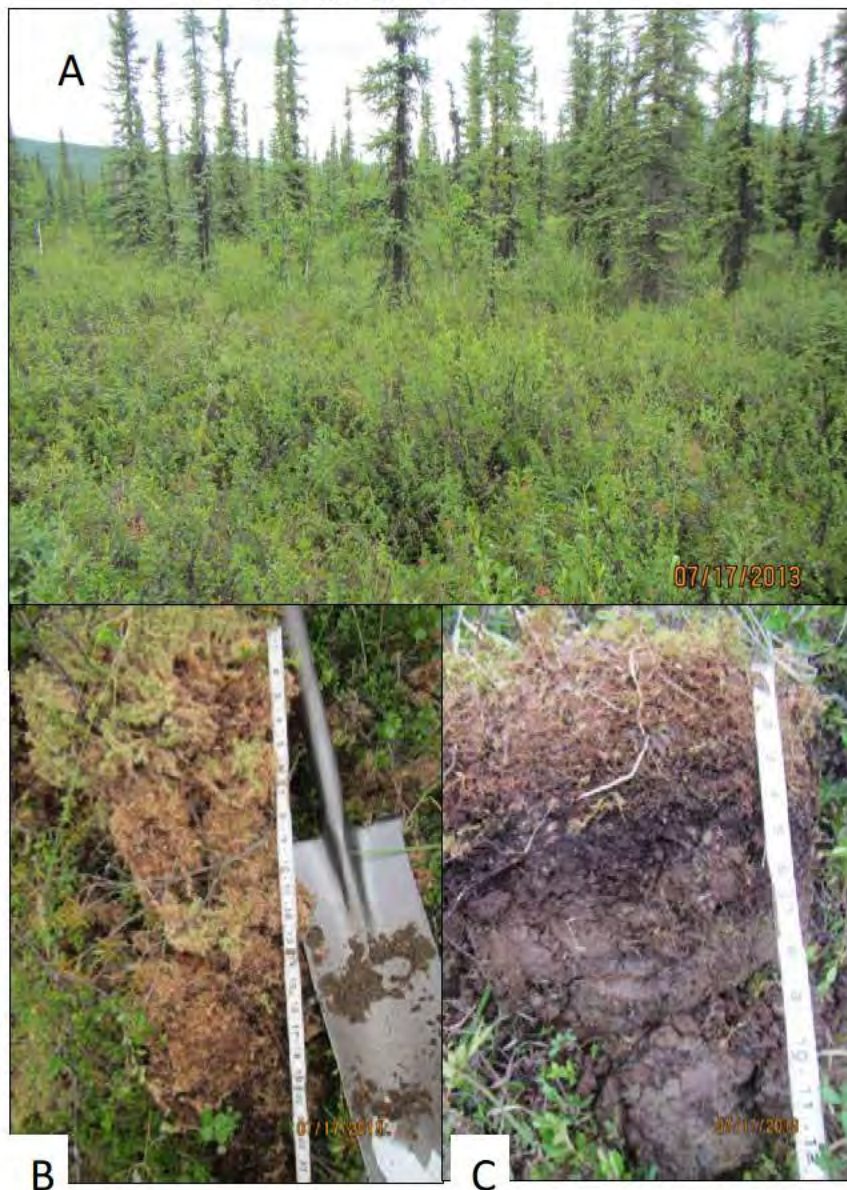
Figure 19. PT research transect (*A*) near-surface soil C, (*B*) N concentrations, and (*C*) soil oxidation–reduction potential results. Note that the sampling locations occurring below the line were chemically reduced during the data collection period.
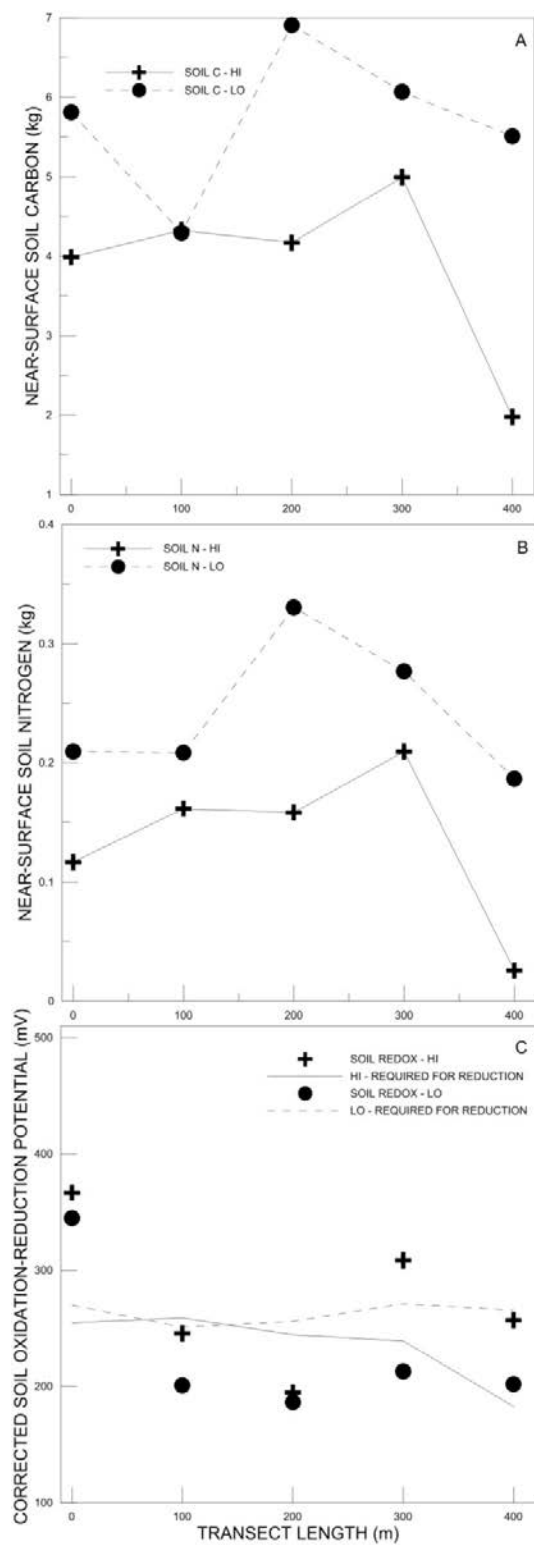
Figure 20. PT research transect (*A*) tree cover, (*B*) average soil moisture (VWC), (*C*) peat layer depth, and (*D*) active-layer depth within LO and HI sampling positions across the research transect. Note that active-layer depth (i.e., the extent of the soil pits) remains deeper in HI sampling positions. Additionally, the depth of all peat layers is deeper in HI sampling positions. VWC generally increases both with depth and in areas lacking tree canopy cover.
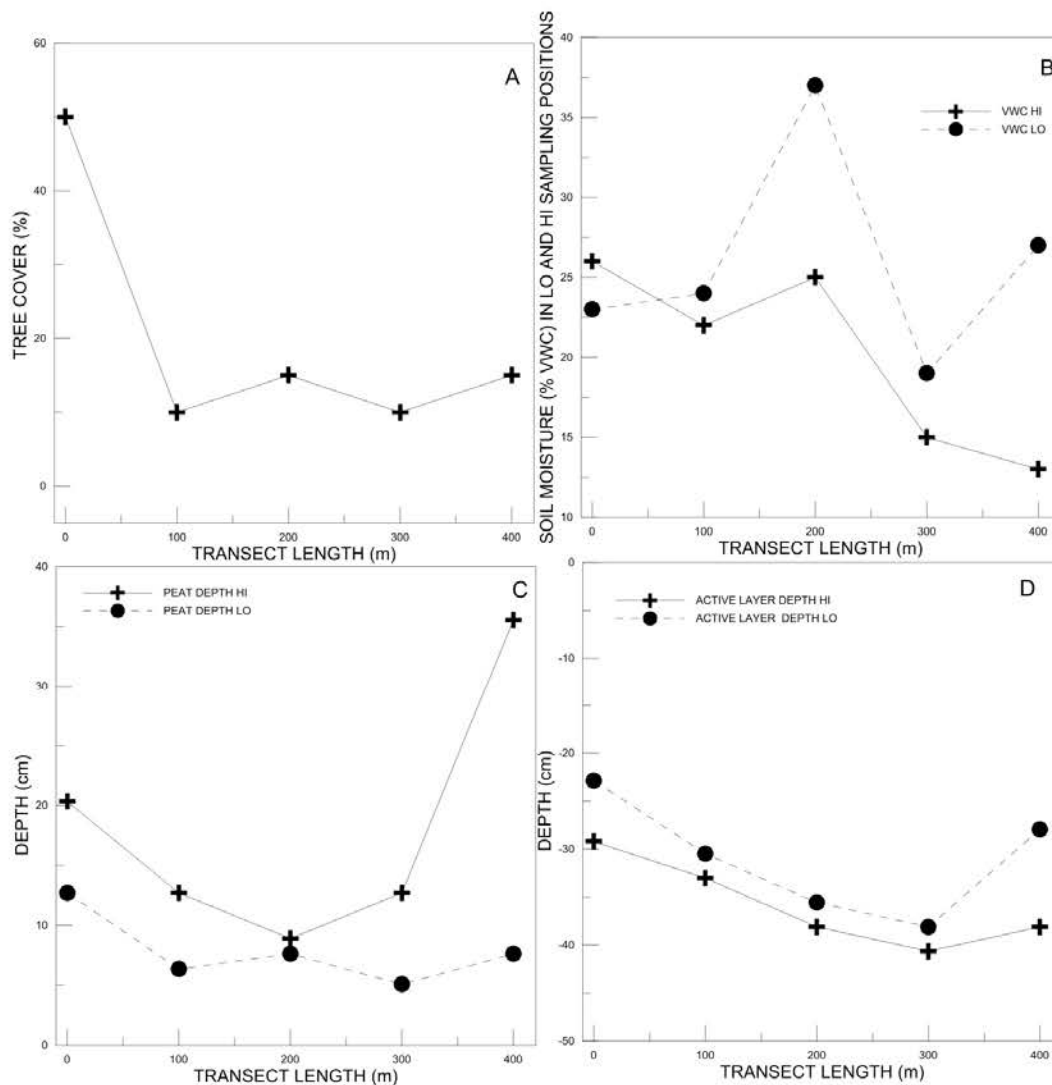
4   Discussion

Results from this study indicate that microtopographic boundary features display distinct soil characteristics. These characteristics can differentiate between landscape positions and therefore have the capacity to aid in identifying permafrost and ground-ice features by using an integrated approach. Notably, peat layers remain significantly thicker (Mann-Whitney U = 46.0; p = 0.006) in microtopographical HI positions, which averaged 18 cm (a range of 7.6–35 cm), compared to LO positions, which averaged 11 cm (a range of 5.1–25 cm), across all three research transects. Sebacher et al. (1986) reported similar peat thicknesses (a range of 5–45 cm) at study sites north of Fairbanks. Understanding factors influencing peat thickness represents a key component to detecting ground conditions and predicting future soil stability as disturbances to peat layers (e.g., fire, forest clearing, erosion, flooding, and climate warming) lead to permafrost and landscape degradation (Davis 2001; Myers-Smith et al. 2007; Douglas et al. 2008).

The thickness of the active-layer was significantly greater in microtopographic HI positions (U = 50.0; p = 0.009) and decreased at topographic boundaries. In the HI positions, active layers ranged from 27 to 64 cm (averaging 37 cm); LO topographic positions ranged from 22 to 48 cm (averaging 30 cm). Viereck (1982) reported similar active-layer thicknesses in Interior Alaska with results ranging from 40 to 50 cm. Zona et al. (2011) also found significantly deeper active-layer thaw depths associated with low microtopographic locations although that study examined ice-rich areas displaying clear polygonal ground features. Notably, Nelson et al. (1997) used field measurements and GIS (geographic information system) tools to estimate active-layer thickness over a large area (greater than 26,000 km²) in north central Alaska. These two studies highlight utility in coupling ground-based measures with remote-sensing tools in the evaluating permafrost features at large spatial scales.

Soil oxidation–reduction measurements were significantly different—ANOVA $F(1,28)$ = 7.80; p = 0.009—with lower redox potentials occurring in LO sampling locations. Redox-potential measurements in reduced soils ranged from 65 to –143 mV across all three field sites. Rivkina et al. (1998) reported similar results with anaerobic conditions between 40 and

−256 mV in permafrost soils from Russia. LO sampling positions also displayed significantly higher volumetric water content—$F(1,27) = 5.07$; $p = 0.033$. Zona et al. (2011) reported similar results with microtopographic low positions displaying significantly lower redox potentials and soil moisture values. Soil moisture plays a key role in the regulation of many ecological processes and interactions in arctic regions (Boike et al. 1998; Romanovsky et al. 2002), and the presence or absence of permafrost dictates many hydrologic regimes at both local and landscape scales (Yoshikawa and Hinzman 2003). A number of remote-sensing techniques (e.g., passive microwave techniques) measure soil moisture, allowing for landform delineation at large spatial scales (Njoku and Entekhabi 1996; Zhang et al. 2003). Our findings suggest that ground-based measures of soil moisture and redox could be used in an integrated approach for detecting and monitoring permafrost and ice features.

This preliminary investigation of near-surface soil nutrients indicated that the majority of samples analyzed exhibited higher nutrient levels in LO topographic locations. Across all three field sites, soil C stocks were greater in LO sample locations—$F(1,28) = 7.96$; $p = 0.009$. This increased soil C coupled with the observed decrease in redox potentials indicates C accumulation and lower rates of aerobic microbial respiration associated with chemically reduced soil conditions (Reddy and DeLaune 2008). Zona et al. (2011) also reported increased organic matter C in low topographic positions. Measured concentrations of soil N produced similar results with N concentrations being significantly greater ($U = 51.1$; $p = 0.010$) in LO microtopographic positions. Fully integrating these results into a geophysical and remote-sensing approach for permafrost and ground-ice detection will require additional research at the microtopographic scale.

Vegetative communities displayed several trends regarding soil characteristics across each of the three research transects. For example, soil moisture increased in areas with limited tree canopy cover. These findings agree with established relationships between vegetative processes (e.g., evapotranspiration) and soil properties (e.g., water holding capacity). Across the research transects, areas with decreased tree cover generally contained thicker surface peat layers and shallower active-layer thaw depths. The relationships between tree cover, microtopography, soils, and ground-ice conditions require additional research. There is promise that standoff detection capabilities can be developed that use changes in soil surface moisture, vegetation, and/or topographic characteristics to "map"

permafrost ice content or permafrost soil composition. The results presented here suggest existing associations are capable of guiding the development and deployment of remote-sensing and geophysical tools to support an integrated approach to permafrost delineation.

5   Opportunities for Future Research

The current dataset demonstrates the potential for using key landscape features in identifying permafrost features. However, a more intensive data collection effort is required to better define boundary areas and the ability of ground-based microtopographic relief to support permafrost delineation, particularly when coupling the data to remote-sensed imaging or spectra. Because of the time constraints of the project, we examined only the active (i.e., seasonally thawed) layer, providing a snapshot of current conditions within the study area. Additional data collected throughout the growing season would provide a more comprehensive picture of boundary characteristics and shifts in plant and soil attributes during the year. Project collaborators have conducted seasonal frost probing, making additional transect data available for analysis. Further research examining changes within the soil and vegetative community along microtopographic gradients would provide a platform for studying the effects of landscape disturbances (e.g., road building) and climate change on areas containing permafrost and ground ice. Previous studies have shown that landscape changes and shifts in climatic conditions have significant effects on soil properties, including C sequestration and biogeochemical cycling. The current study design provides an excellent basis for continuing work in these areas.

6   Conclusions

The current report examined soil and vegetative characteristics across three research transects located near Fairbanks, AK. Results demonstrate the ability of soil characteristics to differentiate microtopographic features in areas containing discontinuous permafrost and ground-ice features. Significant differences observed along a microtopographic gradient include peat depth, active-layer depth, soil oxidation–reduction potential, soil moisture, and soil C and N concentrations. The findings presented correspond to results from other studies although few sources focus on the effect of microtopography on ground characteristics, especially in discontinuous permafrost regions. Developing efficient tools for the delineation of permafrost and ground-ice features requires further research to link these field observations with remotely sensed data.

References

Allison, S. D., and K. K. Treseder. 2011. Climate change feedbacks to microbial decomposition in boreal soils. *Fungal Ecology* 4 (6): 362–374.

Boike, J., K. Roth, and P. P. Overduin. 1998. Thermal and hydrological dynamics of the active layer at continuous permafrost site (Taymyr Peninsula, Siberia). *Water Resources Research* 34:355–363.

Chapman, W. L., and J. E. Walsh. 2007. Simulations of Arctic temperature and pressure by global coupled models. *Journal of Climate* 20 (4): 609–632.

Chester, E. W., B. E. Wofford, and R. Kral. 1997. Atlas of Tennessee Vascular Plants. Vol. 2. Miscellaneous Publication No. 13. Clarksville, TN: Austin Peay State University.

Chorover, J., R. Kretzschmar, F. Garcia-Pichel, and D. Sparks. 2007. Surface biogeochemical processes within the critical zone. *Elements* 3:321–326.

Davis, N. 2001. *Permafrost, A Guide to Frozen Ground in Transition*. Fairbanks, AK: University of Alaska Fairbanks.

Davidson, E. A., and I. A. Janssens. 2006. Temperature sensitivity of soil carbon decomposition and feedbacks to climate change. *Nature* 440 (7081): 165–173.

Douglas, T. A., M. T. Jorgenson, M. Z. Kanevskiy, V. E. Romanovsky, Y. Shur, and K. Yoshikawa. 2008. Permafrost dynamics at the Fairbanks Permafrost Experimental Station near Fairbanks, Alaska. In *Proceedings of the Ninth International Conference on Permafrost*, 28 June–3 July, 373–378.

Douglas, T. A., J. D. Blum, L. Guo, K. Keller, and J. D. Gleason. 2013. Hydrogeochemistry of seasonal flow regimes in the Chena River, a subarctic watershed draining discontinuous permafrost in interior Alaska (USA). *Chemical Geology* 335:48–62.

Douglas, T. A., M.C. Jones, C. A. Hiemstra, and J. Arnold. 2014. Sources and sinks of carbon in boreal ecosystems of Interior Alaska: A review. *Elementa: Science of the Anthropocene* 2:000032. doi:10.12952/journal.elementa.000032.

Eilers, L. J., and D. M. Roosa. 1991. *The Vascular Plants of Iowa*. Iowa City, IA: University of Iowa Press.

Elias, T. E. 1980. *The Complete Trees of North America—Field Guide and Natural History*. New York, NY: Van Nostrand Reinhold Co.

Engstrom, R., A. Hope, H. Kwon, D. Stow, and D. Zamolodchikov. 2005. Spatial distribution of near surface soil moisture and its relationship to microtopography in the Alaskan Arctic Coastal Plain. *Nordic hydrology* 36:219–234.

Etzelmüller, B., R. S. Ødegård, I. Berthling, and J. L. Sollid. 2001. Terrain parameters and remote sensing data in the analysis of permafrost distribution and periglacial processes: principles and examples from southern Norway. *Permafrost and Periglacial Processes* 12 (1): 79–92.

Faulkner, S. P., W. H. Patrick, and R. P. Gambrell. 1989. Field techniques for measuring wetland soil parameters. *Soil Science Society of America Journal* 53 (3): 883–890.

Fisher, J. P., C. Estop-Aragones, G. Xenakis, I. P. Hartley, J. Murton, D. Charman, and G. K. Phoenix. 2013. Influence of Plant Communities on Active Layer Depth in Unburned and Post-fire Forest. In *AGU Fall Meeting Abstracts* 1:0508.

Furlow, J. J. 1997. Betulaceae. In *Flora of North America North of Mexico*, ed. Flora of North America Editorial Committee, 3:509–538.

Goffinet, B., W. R. Buck, and A. J. Shaw. 2008. Morphology and Classification of the Bryophyta. In *Bryophyte Biology*, ed. B. Goffinet and J. Shaw, 55–138. 2nd ed. New York, NY: Cambridge University Press.

Johnson, K. D., J. Harden, A. D. McGuire, N. B. Bliss, J. G. Bockheim, et al. 2011. Soil carbon distribution in Alaska in relation to soil-forming factors. *Geoderma* 167–168:71–84.

Jorgenson, M. T., C. H. Racine, J. C. Walters, and T. E. Osterkamp. 2001. Permafrost degradation and ecological changes associated with a warming climate in central Alaska. *Climatic change* 48 (4): 551–579.

Jorgenson, M. T., Y. L. Shur, and E. R. Pullman. 2006. Abrupt increase in permafrost degradation in Arctic Alaska. *Geophysical Research Letters* 33 (2).

Jorgenson, M. T., and T. E. Osterkamp. 2005. Response of boreal ecosystems to varying modes of permafrost degradation. *Canadian Journal of Forest Research* 35 (9): 2100–2111.

Jorgenson, M. T., V. Romanovsky, J. Harden, Y. Shur, J. O'Donnell, E. A. G. Schuur, M. Kanevskiy, and S. Marchenko. 2010. Resilience and vulnerability of permafrost to climate change. *Canadian Journal of Forest Research* 40 (7): 1219–1236.

Kääb, A. 2008. Remote sensing of permafrost-related problems and hazards. *Permafrost and Periglacial Processes* 19 (2): 107–136.

Kahn, L. 1988. *Determination of Total Organic Carbon in Sediment (Lloyd Kahn Method)*. Edison, NJ: U.S. Environmental Protection Agency, Region II, Environmental Services Division.

Klute A. 1986. *Methods of Soil Analysis: Part 1—Physical and Mineralogical Methods.* 3rd ed. Madison, WI: Soil Science Society of America Press.

Lichvar, R. W., M. Butterwick, N. C. Melvin, and W. R. Kirchner. 2014. The National Wetland Plant List: 2014 Update of Wetland Ratings. *Phytoneuron* 2014-41:1–42.

Lipson, D. A., D. Zona, T. K. Raab, F. Bozzolo, M. Mauritz, W. C. Oechel. 2012. Water table height and microtopography control Biogeochemical cycling in an Arctic coastal tundra Ecosystem. *Biogeosciences* 9:577–591.

Pojar, J., A. MacKinnon. 1994. *Plants of the Pacific Northwest Coast: Washington, Oregon, British Columbia and Alaska.* Auburn, WA: Lone Pine Publishing.

Marchenko, S., V. Romanovsky, and G. Tipenko. 2008. Numerical modeling of spatial permafrost dynamics in Alaska. In *Proceedings of the Ninth International Conference on Permafrost.* Fairbanks, AK: Institute of Northern Engineering, University of Alaska Fairbanks.

Myers-Smith, I. H., A. D. McGuire, J. W. Harden, and F. S. Chapin. 2007. Influence of disturbance on carbon exchange in a permafrost collapse and adjacent burned forest. *Journal of Geophysical Research: Biogeosciences* 112 (G4): G04017.

Natural Resources Conservation Service. 2002. *Plant Fact Sheet—American Cranberrybush.* Washington, DC: U.S. Department of Agriculture. http://plants.usda.gov/factsheet/pdf/fs_viopa2.pdf.

Nelson, F. E., N. I. Shiklomanov, G. R. Mueller, K. M. Hinkel, D. A. Walker, and J. G. Bockheim. 1997. Estimating active-layer thickness over a large region: Kuparuk River basin, Alaska, USA. *Arctic and Alpine Research* 29 (4): 367–378.

Njoku, E. G., and D. Entekhabi. 1996. Passive microwave remote sensing of soil moisture. *Journal of hydrology* 184 (1): 101–129.

Osterkamp, T., and J. Jorgenson. 2006. Warming of permafrost in the Arctic National Wildlife Refuge, Alaska. *Permafrost Periglacial Process* 17 (1): 65–69.

Peterson, K. M., and W. D. Billings. 1980. Tundra vegetational patterns and succession in relation to microtopography near Atkasook, Alaska. *Arctic and Alpine Research* 12 (4): 473–482.

Potter, C. 2004. Predicting climate change effects on vegetation, soil thermal dynamics, and carbon cycling in ecosystems of interior Alaska. *Ecological Modelling* 175 (1): 1–24.

Racine, C. H., J. C. Walters, and M. T. Jorgenson. 1998. Airboat Use and Disturbance of Floating Mat Fen Wetlands in Interior Alaska, U.S.A. *Arctic* 51 (4): 371–377.

Radford, A. E., H. E. Ahles, and C. R. Bell. 1968. *Manual of the Vascular Flora of the Carolinas.* Chapel Hill, NC: University of North Carolina Press.

Reddy, K. R., and R. D. DeLaune. 2008. *Biogeochemistry of Wetlands: Science and Applications.* Boca Raton, FL: CRC Press.

Rivkina, E., D. Gilichinsky, S. Wagener, J. Tiedje, and J. McGrath. 1998. Biogeochemical activity of anaerobic microorganisms from buried permafrost sediments. *Geomicrobiology Journal* 15 (3): 187–193.

Romanovsky, V. E., M. Burgess, S. Smith, K. Yoshikawa, and J. Brown. 2002. Permafrost Temperature Records: Indicators of Climate Change. *Eos* 83 (50): 586–594.

Schuur, E. A., J. Bockheim, J. G. Canadell, E. Euskirchen, C. B. Field, S. V. Goryachkin, and S. A. Zimov. 2008. Vulnerability of permafrost carbon to climate change: Implications for the global carbon cycle. *BioScience* 58 (8): 701–714.

Segers, R. 1998. Methane production and methane consumption: a review of processes underlying wetland methane fluxes. *Biogeochemistry* 41:23–51.

Sebacher, D. I., R. C. Harriss, K. B. Bartlett, S. M. Sebacher, and S. S. Grice. 1986. Atmospheric methane sources: Alaskan tundra bogs, an alpine fen, and a subarctic boreal marsh. *Tellus B* 38 (1): 1–10.

Sierra, C. A., M. E. Harmon, E. Thomann, S. S. Perakis, H. W. Loescher. 2011. Amplification and dampening of soil respiration by changes in temperature variability. *Biogeosciences* 8: 951–961.

Sparks, D. L., A. L. Page, P. A. Helmke, R. H. Loeppert, P. N. Soltanpour, M. A. Tabatabai, C. T. Johnston, M. E. Sumner. 1996. Redox measurements of soils. In *Methods of Soil Analysis. Part 3—Chemical Methods*, 1255–1273. Madison, WI: Soil Science Society of America, Inc.

IBM Corp. 2011. IBM SPSS for Windows, Version 20.0. Armonk, NY: IBM Corp.

Stow, D. A., A. Hope, D. McGuire, D. Verbyla, J. Gamon, F. Huemmrich, et al. 2004. Remote sensing of vegetation and land-cover change in Arctic Tundra Ecosystems. *Remote Sensing of Environment* 89 (3): 281–308.

Tarnocai, C., and I. Campbell. 2002. Soils of the polar regions. In *Encyclopedia of Soil Science*, 1018–1021. New York, NY: Marcel Dekker.

U.S. Army Corps of Engineers (USACE). 2007. *Regional Supplement to the Corps of Engineers Wetland Delineation Manual: Alaska Region (Version 2.0)*, ed. J. S. Wakeley, R. W. Lichvar, and C. V. Noble. ERDC/EL TR-07-24. Vicksburg, MS: U.S. Army Engineer Research and Development Center.

U.S. Department of Agriculture (USDA), Natural Resources Conservation Service (NRCS). 2014. *The PLANTS Database*. Greensboro, NC: National Plant Data Team. http://plants.usda.gov (accessed 15 August 2014).

Vepraskas, M. J., and S. P. Faulkner. 2001. Redox chemistry of hydric soils. In *Wetland Soils: Genesis, Hydrology, Landscapes, and Classification*, ed. J. L. Richardson and M. J. Vepraskass, 85–106.

Viereck, L. A. 1982. Effects of fire and firelines on active layer thickness and soil temperatures in interior Alaska. In *Proceedings of the Fourth Canadian Permafrost Conference*, 123–135. Ottawa, Canada: National Research Council of Canada.

Walker, M. D., C. H. Wahren, R. D. Hollister, G. H. Henry, L. E. Ahlquist, et al. 2006. Plant community responses to experimental warming across the tundra biome. In *Proceedings of the National Academy of Sciences of the united States of America* 103 (5): 1342–1346. doi:10.1073/pnas.0503198103.

Williams, P. J., and M. W. Smith. 1989. Hydrology of Frozen Ground. In *The Frozen Earth*, 202–236. Studies in Polar Research. Cambridge, UK: Cambridge University Press.

Wolken, J. M., T. N. Hollingsworth, T. S. Rupp, F. S. Chapin III, S. F. Trainor, et al. 2011. Evidence and implications of recent and projected climate change in Alaska's forest ecosystems. *Ecosphere* 2 (11): art124.

Yoshikawa, K., and L. D. Hinzman. 2003. Shrinking thermokarst ponds and groundwater dynamics in discontinuous permafrost near Council, Alaska. *Permafrost and Periglacial Processes* 14 (2): 151–160.

Zhang, T., R. G. Barry, K. Knowles, F. Ling, and R. L. Armstrong. 2003. Distribution of seasonally and perennially frozen ground in the Northern Hemisphere. In *Proceedings of the 8th International Conference on Permafrost*, ed. M. Phillips, S. M. Springman, and L. U. Arenson, 2:1289–1294. Zurich, Switzerland: A. A. Balkema Publishers.

Zona, D., D. A. Lipson, R. C. Zulueta, S. F. Oberbauer, and W. C. Oechel. 2011. Microtopographic controls on ecosystem functioning in the Arctic Coastal Plain. *Journal of Geophysical Research: Biogeosciences (2005–2012)* 116 (G4): G00I08.

Appendix

Appendix A. List of plants observed within each transect sample point. CF = Creamers Field, FL = Farmers Loop; PT = Permafrost Tunnel.

Common Name	Scientific Name	Indicator Status*	CF	FL	PT	Citation
Alder	*Alnus rubra*	FAC	X	X		Elias (1980)
Dwarf birch	*Betula nana*	FAC	X	X	X	USDA, NRCS (2014)
Paper birch	*Betula neoalaskana*	FACU	X	X	X	Furlow (1997)
Bluejoint	*Calamagrostis canadensis*	FAC	X	X	X	Radford et al. (1968)
Sedge	*Carex* spp.	FACW		X		Radford et al. (1968)
Fireweed	*Chamerion angustifolium*	FACU		X		Radford et al. (1968)
Field hosetail	*Equisetum arvense*	FAC		X		Radford et al. (1968)
Meadow horsetail	*Equisetum pratense*	FACW			X	USDA, NRCS (2014)
Tussock cottongrass	*Eriophorum vaginatum*	FACW	X	X	X	USDA, NRCS (2014)
Strawberry	*Fragaria canadensis*	UPL		X		USDA, NRCS (2014)
Labrador tea	*Rhododendron groenlandicum*	FAC			X	USDA, NRCS (2014)
Twinflower	*Linnaea borealis*	FACU		X		USDA, NRCS (2014)
White spruce	*Picea glauca*	FACU			X	Elias (1980)
Black spruce	*Picea mariana*	FACW	X	X	X	Elias (1980)
Quaking aspen	*Populus tremuloides*	FACU			X	Elias (1980)
Choke cherry	*Prunus virginiana*	FAC	X			Elias (1980)
Prickly rose	*Rosa acicularis*	FACU	X	X		Eilers and Roosa (1991)
Salmonberry	*Rubus spectabilis*	FACU	X	X	X	USDA, NRCS (2014)
Willow	*Salix* spp.	FACW	X	X	X	Elias (1980)
Sphagnum	*Sphagnum* spp.	OBL	X	X	X	Goffinet et al. 2008
Watermelon berry	*Streptopus amplexifolius*	FACU		X		Radford et al. (1968)
Coltsfoot	*Tussilago farfara*	FACU		X	X	Chester et al. (1997)
Blueberry	*Vaccinium alaskaense*	FAC	X	X	X	Pojar and MacKinnon (1994)
Lowbush cranberry	*Viburnum trilobum*	FAC	X	X	X	Natural Resources Conservation Service (2002)
Highbush cranberry	*Vaccinium oxycoccos*	FACW		X		Natural Resources Conservation Service (2002)

* The indicator status indicates a species' preference for growing in wetlands or uplands. OBL = Obligate Wetland; FACW = Facultative Wetland; FAC = Facultative; FACU = Facultative Upland; UPL = Obligate Upland

REPORT DOCUMENTATION PAGE			*Form Approved* OMB No. 0704-0188
Public reporting burden for this collection of information is estimated to average 1 hour per response, including the time for reviewing instructions, searching existing data sources, gathering and maintaining the data needed, and completing and reviewing this collection of information. Send comments regarding this burden estimate or any other aspect of this collection of information, including suggestions for reducing this burden to Department of Defense, Washington Headquarters Services, Directorate for Information Operations and Reports (0704-0188), 1215 Jefferson Davis Highway, Suite 1204, Arlington, VA 22202-4302. Respondents should be aware that notwithstanding any other provision of law, no person shall be subject to any penalty for failing to comply with a collection of information if it does not display a currently valid OMB control number. **PLEASE DO NOT RETURN YOUR FORM TO THE ABOVE ADDRESS.**			

1. REPORT DATE *(DD-MM-YYYY)* August 2015	**2. REPORT TYPE** Technical Report/Final	**3. DATES COVERED** *(From - To)*

4. TITLE AND SUBTITLE Investigation of Soil and Vegetation Characteristics in Discontinuous Permafrost Landscapes Near Fairbanks, Alaska	**5a. CONTRACT NUMBER**
	5b. GRANT NUMBER
	5c. PROGRAM ELEMENT NUMBER
6. AUTHOR(S) Jacob F. Berkowitz, Christopher A. Hiemstra, and Thomas A. Douglas	**5d. PROJECT NUMBER**
	5e. TASK NUMBER
	5f. WORK UNIT NUMBER

7. PERFORMING ORGANIZATION NAME(S) AND ADDRESS(ES) Cold Regions Research and Engineering Laboratory (CRREL) U.S. Army Engineer Research and Development Center (ERDC) 72 Lyme Road Hanover, NH 03755-1290	**8. PERFORMING ORGANIZATION REPORT NUMBER** ERDC TR-15-7

9. SPONSORING / MONITORING AGENCY NAME(S) AND ADDRESS(ES) Headquarters, U.S. Army Corps of Engineers Washington, DC 20314-1000	**10. SPONSOR/MONITOR'S ACRONYM(S)**
	11. SPONSOR/MONITOR'S REPORT NUMBER(S)

12. DISTRIBUTION / AVAILABILITY STATEMENT
Approved for public release; distribution is unlimited.

13. SUPPLEMENTARY NOTES

ERDC Center-Directed Research project "Integrated Technologies for Delineating Permafrost and Ground-State Conditions"

14. ABSTRACT

Alaska contains large areas of discontinuous permafrost, yet few studies examine the impact of microtopography on ground conditions and permafrost stability. This report uses vegetation and soil measurements to identify statistically significant differences to potentially classify permafrost ground-state conditions. The study identified significant relationships between soil parameters and vegetative community structure, including thicker peat layers in high microtopographic positions, greater active-layer thaw depths in high microtopographic positions, increased redox potentials in elevated microtopographic positions, and decreased soil moisture in higher topographic locations. Additionally, soil carbon and nitrogen concentrations increased in low microtopographic positions. These results suggest that soil and vegetation conditions may provide useful proxy measures in identifying permafrost and ground-ice features when incorporated into an integrated approach that combines belowground geophysics with aboveground remotely sensed terrain characteristics. Additional research is needed to combine soil and vegetation characteristics with suborbital and satellite-based remotely sensed measurements, such as airborne LiDAR, spectral reflectance, and high-resolution ground-level subsidence measurements.

15. SUBJECT TERMS Active-layer depth Discontinuous permafrost	Ground-ice features Interior Alaska Microtopography	Permafrost stability Soil nutrients Vegetation

16. SECURITY CLASSIFICATION OF:			**17. LIMITATION OF ABSTRACT**	**18. NUMBER OF PAGES**	**19a. NAME OF RESPONSIBLE PERSON**
a. REPORT Unclassified	**b. ABSTRACT** Unclassified	**c. THIS PAGE** Unclassified	SAR	50	**19b. TELEPHONE NUMBER** *(include area code)*